


# Nitrogen deposition outweighs climatic variability in driving annual growth rate of canopy beech trees: Evidence from long-term growth reconstruction across a geographic gradient

Tiziana Gentilesca<sup>1</sup> | Angelo Rita<sup>1</sup> | Michele Brunetti<sup>2</sup> | Francesco Giammarchi<sup>3</sup> | Stefano Leonardi<sup>4</sup> | Federico Magnani<sup>5</sup> | Twan van Noije<sup>6</sup> | Giustino Tonon<sup>3</sup> | Marco Borghetti<sup>1</sup> 

<sup>1</sup>Scuola di Scienze Agrarie, Forestali, Alimentari ed Ambientali, Università della Basilicata, Potenza, Italy

<sup>2</sup>Istituto di Scienze dell'Atmosfera e del Clima, Consiglio Nazionale delle Ricerche, Bologna, Italy

<sup>3</sup>Faculty of Science and Technology, Free University of Bolzano, Bolzano, Italy

<sup>4</sup>Dipartimento di Scienze Chimiche, della Vita e della Sostenibilità Ambientale, Università di Parma, Parma, Italy

<sup>5</sup>Dipartimento di Scienze Agrarie, Università di Bologna, Bologna, Italy

<sup>6</sup>Royal Netherlands Meteorological Institute (KNMI), AE De Bilt, The Netherlands

## Correspondence

Marco Borghetti, Scuola di Scienze Agrarie, Forestali, Alimentari ed Ambientali, Università della Basilicata, Potenza, Italy.  
Email: marco.borghetti@unibas.it

## Funding information

MIUR-PRIN, Grant/Award Number: 2012E3F3LK

## Abstract

In this study, we investigated the role of climatic variability and atmospheric nitrogen deposition in driving long-term tree growth in canopy beech trees along a geographic gradient in the montane belt of the Italian peninsula, from the Alps to the southern Apennines. We sampled dominant trees at different developmental stages (from young to mature tree cohorts, with tree ages spanning from 35 to 160 years) and used stem analysis to infer historic reconstruction of tree volume and dominant height. Annual growth volume ( $G_V$ ) and height ( $G_H$ ) variability were related to annual variability in model simulated atmospheric nitrogen deposition and site-specific climatic variables, (i.e. mean annual temperature, total annual precipitation, mean growing period temperature, total growing period precipitation, and standard precipitation evapotranspiration index) and atmospheric  $CO_2$  concentration, including tree cambial age among growth predictors. Generalized additive models (GAM), linear mixed-effects models (LMM), and Bayesian regression models (BRM) were independently employed to assess explanatory variables. The main results from our study were as follows: (i) tree age was the main explanatory variable for long-term growth variability; (ii) GAM, LMM, and BRM results consistently indicated climatic variables and  $CO_2$  effects on  $G_V$  and  $G_H$  were weak, therefore evidence of recent climatic variability influence on beech annual growth rates was limited in the montane belt of the Italian peninsula; (iii) instead, significant positive nitrogen deposition ( $N_{dep}$ ) effects were repeatedly observed in  $G_V$  and  $G_H$ ; the positive effects of  $N_{dep}$  on canopy height growth rates, which tended to level off at  $N_{dep}$  values greater than approximately  $1.0 \text{ g m}^{-2} \text{ y}^{-1}$ , were interpreted as positive impacts on forest stand above-ground net productivity at the selected study sites.

## KEYWORDS

age, climate change, *Fagus sylvatica* L, forest, height growth, nitrogen deposition, stem analysis, volume growth

## 1 | INTRODUCTION

Anthropogenic climate change, triggered by a rise in greenhouse gases, and atmospheric nitrogen (N) deposition, fostered by N emissions from fuel combustion and intensive agriculture, have potential to result in relevant consequences on the function and productivity of forest ecosystems (Churkina et al., 2010; IPCC, 2014). Understanding the impacts under global change conditions is pivotal knowledge, as this information will likely serve to shape forests that better meet carbon store objectives and wood demands; however, these objectives present challenges due to the interactions between the environmental drivers of forest growth and functional feedbacks in the long-term (Boisvenue & Running, 2006; Hyvönen et al., 2007).

A range of studies recorded increased forest growth and carbon accumulation in recent decades for many temperate and boreal forests over large geographic areas (e.g. Ciais et al., 2008; Pretzsch, Biber, Schütze, Uhl, & Rötzer, 2014; Spiecker, 1995; Spiecker, Mielikäinen, Köhl, & Skovsgaard, 1996). Enhanced forest productivity was variously attributed to changes in environmental conditions (e.g. increased atmospheric CO<sub>2</sub> concentrations, extended growing season as a consequence of climate warming, and fertilization due to N deposition), however, anthropic pressure reductions on timber extraction and major reshaping in forest management are also likely to play a role through substantial effects on site fertility; see Kahle et al. (2008) for a summary of results from the Recognition project on growth trends in European forests.

Approximately  $18 \times 10^9$  kg of N are globally deposited in forests each year, with large regional differences in annual deposition rates among regions and forest types (Leonardi, Magnani, Nolè, Van Noije, & Borghetti, 2015; Schlesinger, 2009). For this reason, nitrogen deposition (N<sub>dep</sub>) impacts on forest productivity were the subject of a range of studies (Hyvönen et al., 2007; Schulte-Uebbing & de Vries, 2017; Solberg et al., 2004; de Vries, Reinds, Guinderson, & Sterba, 2006), with a lively scientific debate on the relevance and magnitude of the N<sub>dep</sub> response, particularly following a paper by Magnani et al. (2007), where results showed a strong relationship between N<sub>dep</sub> and net ecosystem production in temperate and boreal forests (Magnani et al., 2008; de Vries et al., 2008). Subsequently, Solberg et al. (2009) reported a response of forest growth to N availability from a synchronic analysis of forest plots established throughout Europe to monitor air pollution effects on forests (ICP Forests), which suggested a likely cause-effect relationship between N<sub>dep</sub> and forest growth, particularly for pine and spruce. In this synchronic approach, large spatial variability was considered, assessment of single predictor effects was challenging, and some environmental effects remained uncertain; see also de Vries, Dobbertin, Solberg, Van Dobbers, and Schaub (2014) and Schulte-Uebbing and de Vries (2017) for review and meta-analysis. Cienciala et al. (2016) showed similar results on forest growth sensitivity to N<sub>dep</sub> based on a comparison of forest inventory plots. Other studies provided useful insights regarding forest growth response to N<sub>dep</sub>; however, the data were restricted to radial

increments (Hess et al., 2018; Kint et al., 2012) or were based on short-term experimental approaches, which neglected age-effects on tree growth (e.g. Ferretti et al., 2014; Gentilesca, Vieno, Perks, Borghetti, & Mencuccini, 2013) or annual variability in N<sub>dep</sub> was not included to interpret annual growth variation (Bontemps, Hervé, Leban, & Dhôte, 2011).

A diachronic study in which the relationship between long-term annual forest growth rates, annual variability in climatic variables, and annual nitrogen deposition rates is explored at a range of sites under different nitrogen loads is not yet available. Current evidence indicates N<sub>dep</sub> might have limited effects in areas with chronic or high N<sub>dep</sub> levels (Aber, McDowell, & Nadelhoffer, 1998; Gentilesca et al., 2013), whereas a positive effect on forest growth might be expected in areas with low to medium N<sub>dep</sub> (Vadeboncoeur, 2010).

Reconstruction of past forest growth is a useful and widely applied approach to explore potential forest response to changes in environmental conditions. Long-term growth trends were often obtained by tree ring analyses, however, radial growth strongly depends on competition among trees and is therefore sensitive to natural or management-induced disturbances. Growth analysis of canopy dominant trees and retrospective reconstruction of stem volume and height growth rates by stem analysis is a time-consuming approach, however, it is important to obtain reliable long-term trends in forest productivity and interpretation of environmental effects on forest growth (see Bontemps, Hervé, & Dhôte, 2009, 2010, for review and application).

In this work, we studied canopy trees in common beech (*Fagus sylvatica* L.) forests across a regional transect in the montane belt of the Italian peninsula, where a range of climatic conditions and nitrogen deposition rates were examined. We generated an historical reconstruction of tree volume and dominant height with the objective of resolving the role of climatic variables and N<sub>dep</sub> in driving aboveground forest productivity. For this purpose, we used historical model simulated N<sub>dep</sub> and *ad hoc* generated synthetic records of monthly temperature and precipitation series, reconstructed to be representative of the specific forest sample sites. In particular, our objective was to answer the following questions: (i) is there a direct human footprint on the annual growth of canopy beech trees due to N<sub>dep</sub> and is the N<sub>dep</sub> effect consistent at sites under different N loads?; and (ii) is a clear sign of climatic variability evident on beech growth at the selected sites or might the response to single climatic variables, (e.g. higher assimilation rates as the primary CO<sub>2</sub> response, increased growing season length as the main temperature response) be masked by functional feedbacks and outweighed by the effects of increased N-availability? Common beech was chosen as a model species due to its ecological and economical importance and the species' reported sensitivity to climate change, particularly towards its geographic limit in southern Europe, where beech growth and competitiveness were considered limited by increased drought and warming temperatures (Jump, Hunt, & Peñuelas, 2006; Piovesan, Biondi, Di Filippo, Alessandrini, & Maugeri, 2008).

## 2 | MATERIALS AND METHODS

### 2.1 | Study sites, tree sampling, and stem analysis

Beech-dominated forests were selected at four sites along a latitudinal transect across the Italian peninsula, distributed over the natural range of beech in Italy, from the Eastern Alps to Southern Apennines; at these sites forests span the so-called European beech to the Mediterranean beech forest types (Pignatti, 1998), experience a wide range of climatic conditions, and different N-loads from long-term  $N_{\text{dep}}$  (Table 1). Forests with a well-documented management history were chosen, with similar structural characteristics at sites where beech grows under favorable climatic and soil conditions (Tables S1, S2 and Figure S1 in Supplementary Information).

In each forest, three even-aged tree cohorts at different developmental stages, from young to mature, were identified based on descriptions available in forest management plans. In each cohort, 8–10 dominant trees forming the main canopy and having comparatively well-developed crowns were visually selected, located at least 20 m apart from each other, and subsequently marked. For each selected tree, we checked growth was not suppressed over the tree's entire life. This was conducted by extracting two perpendicular wood cores from the stem of each tree at a height of 1.30 m using an increment borer. In the laboratory, tree rings were measured to the nearest 0.01 mm using a tree ring measuring system (LINTAB 6 coupled with TSAP-Win Scientific software, Rinntech, Heidelberg, Germany) and cross-dated using Cofecha software (Holmes, 1983). Ring series were subsequently standardized with Arstan software (Cook, Krusic, Holmes, & Peters, 2007) and growth suppression analysis was performed following Rubino and McCarthy (2004).

Stem analysis was performed on trees sampled that did not exhibit radial growth suppression over their life; data were collected from 34 trees aged 35 to 160 years (Table 1). Sample trees were felled and 3–5 cm thick cross sections were taken every 2–4 m

along the stem; sections were transferred to the laboratory, air-dried, and sanded with increasingly fine sandpaper; annual ring widths were then measured to the nearest 0.01 mm, as described above. Data analyses for historical volume and height reconstruction; and annual stem volume growth ( $G_V$ ) and annual stem height growth ( $G_H$ ) computations were performed using the “tReeglia” package (Basciutto, Cherubini, & Scarascia Mugnozza, 2004) available for the R statistical suite version 3.2.3 (R Development Core Team, 2015).

### 2.2 | Environmental variables

The availability of long and reliable temporal series of meteorological variables, possibly very close to forest sites, is crucial to evaluate the climate-growth relationships. However, global or regional climatological datasets frequently lack of representativeness at the local scale, especially remote sites. Therefore, we reconstructed long-term climatic variability in a more accurate way; specifically, long-term monthly temperature and precipitation series (Table 1) were reconstructed for each site by utilizing the rich data available for Italy and interpolating the climate information provided by weather station data applying the anomaly method (Mitchell & Jones, 2005; New, Hulme, & Jones, 2000), as described in Brunetti et al. (2012). The objective was to obtain the best representative climate reconstruction of the specific sample site locations as possible. The procedure reconstructed independent climatologies (i.e. climatological normals over a given reference period) and anomalies (i.e. departures from given reference period). Given the geographic area, climatologies are often characterized by remarkable spatial gradients, require a high spatial climate station density (even under limited temporal coverage), and a sophisticated interpolation procedure (Brunetti, Maugeri, Nanni, Simolo, & Spinoni, 2014; Crespi, Brunetti, Lentini, & Maugeri, 2018) for reconstruction; anomalies (linked to climate variability) are more coherent and a low spatial density is enough, however, long-term temporal coverage and accurate homogenization (e.g.

**TABLE 1** Study sites: Site1, Serra S. Bruno, CS; Site2, Abriola, PZ; Site3, Pian di Novello, PT; Site4, Cansiglio, BL; latitude-N (Lat) and longitude-E (Long) in decimal degrees, and altitude (m) above sea level (Alt);  $N_{\text{cum}}$  = accumulated N deposition ( $\text{g}/\text{m}^2$ ) in the period 1850–2014;  $\text{Int}_G$  = time interval of tree growth reconstruction;  $\text{Int}_T$  = time interval of temperature reconstruction,  $\text{Int}_P$  = time interval of precipitation reconstruction;  $\text{Int}_{N_{\text{dep}}}$  = time interval of N deposition reconstruction;  $\text{Int}_{\text{ass}}$  = time interval for which the assessment took place in each site;  $n$  = number of sampled trees;  $\text{Age}_R$  = age range (years, min–max) of sampled trees

	Site1	Site2	Site3	Site4
Lat	38.56	40.48	44.10	46.03
Long	16.29	15.75	10.70	12.40
Alt	1050	1380	1300	1150
$N_{\text{cum}}$	36.0	59.6	87.5	100.0
$\text{Int}_G$	1920–2014	1891–2014	1856–2014	1866–2014
$\text{Int}_T$	1881–2014	1901–2014	1865–2014	1865–2014
$\text{Int}_P$	1869–2014	1868–2014	1865–2014	1865–2014
$\text{Int}_{N_{\text{dep}}}$	1850–2014	1850–2014	1850–2014	1850–2014
$\text{Int}_{\text{ass}}$	1920–2014	1901–2014	1865–2014	1866–2014
$n$	7	9	8	10
$\text{Age}_R$	60–95	57–124	35–160	66–149

procedures that remove nonclimatic signals introduced by stations and instrument relocation, changes in measurement practices, and so on) is required. Finally, temperature and precipitation monthly series in absolute values for each sampling site can be obtained by superimposing the two fields. Information about the techniques and their accuracy are provided in Brunetti et al. (2012, 2014), and Crespi et al. (2018); and the spatial distributions of the confidence intervals associated to climate reconstructions are presented in Brunetti et al. (2014), for temperature, and in Crespi et al. (2018), for precipitation. Mean annual temperature ( $T$ ) and total annual precipitation ( $P$ ) were calculated from site-specific reconstructed monthly series; mean temperature ( $T_g$ ) and total precipitation ( $P_g$ ) were also determined for April through July, the period during which most tree growth occurs.

For each site, the monthly Standardized Precipitation Evapotranspiration Index (SPEI) was computed following the algorithm proposed by Vicente-Serrano, Beguería, and López-Moreno (2010) implemented in the "SPEI" R package (Beguería & Vicente-Serrano, 2013). SPEI is a multiscalar drought index that evaluates the balance between precipitation and potential evapotranspiration (PET); the calculation was based on the difference between monthly precipitation data ( $P$ ) and PET, which was estimated using the Thornthwaite equation derived from temperature ( $T$ ) and latitude.

For each site, mean annual total atmospheric reactive nitrogen deposition ( $N_{dep}$ , including both oxidized and reduced reactive components) was retrieved for the 1850–2014 period from the long-term WCRP's Coupled Model Intercomparison Project (CMIP6) forcing datasets (v6.2.2, last release 1st November 2017) available via ESGF at <https://esgf-node.llnl.gov/search/input4mips/>. This is pure model data with a spatial resolution of  $1.9 \times 2^\circ$  (Eyring et al., 2016).

Annual atmospheric  $CO_2$  concentration was obtained from the Monte Cimone observatory dataset ( $44.1938^\circ$  N,  $10.7015^\circ$  E), available for download from the World Data Center for Greenhouse Gases ([http://ds.data.jma.go.jp/gmd/wdcgg/pub/products/cd-rom/dvd\\_07/menu/data.html](http://ds.data.jma.go.jp/gmd/wdcgg/pub/products/cd-rom/dvd_07/menu/data.html)). These data covered 1975–2015;  $CO_2$  concentrations for previous periods were estimated from a regression between Monte Cimone values and those provided by McCarroll and Loader (2004).  $CO_2$  values were assumed the same for all sites in a given year.

For each site, annual environmental predictor values were assigned to each combination of reconstructed growth rates and defined tree cambial ages. Table 1 reports the time interval during which the assessment was performed for each study site.

Dataset is available from the Figshare online repository at <https://doi.org/10.6084/m9.figshare.5982298.v1>.

### 2.3 | Statistical procedures

Generalized additive mixed models (GAM) were applied using the "mgcv" library available in the R statistical suite version 3.2.3 (R Development Core Team, 2015) to inspect the shape of stem volume ( $G_V$ ) and stem height ( $G_H$ ) growth response curves to tree age and environmental predictors. GAMs are nonlinear and

nonparametric regression techniques that do not require *a priori* functional relationship specifications between dependent and independent variables. The model strength is the production of link functions to establish a relationship between the response variable mean and a smoothed function of each explanatory variable (Hastie & Tibshirani, 1990; Wood, 2006). A random intercept, considering correlations among trees within sites, was included in the model.

We also predicted tree age and environmental variable effects on  $G_V$  and  $G_H$  by fitting a linear mixed-effects model (LMM), using the library "nlme" available in the R statistical suite.

Initially, we entered all variables with their interactions as fixed-effects into the model (full model). Following Schielzeth (2010), fixed terms were centered and scaled to improve parameter estimates and allow direct comparisons of the regression coefficients. A random effect was included in the model to account for variability among trees within the same site; maximum-likelihood method (ML) and restricted maximum-likelihood method (REML) were, respectively, applied to estimate fixed-effects terms and optimal random structure. Residual error variance and correlation structure were explicitly integrated in the models to include measurement heterogeneity and independence.

Subsequently, a "reduced" model was obtained by performing an automatic backward/forward elimination of full model fixed terms (Burnham & Anderson, 2002). The "stepAIC" function in R library "MASS" was used to determine the best models: stepAIC begins with the full LMM model and sequentially removes and re-combines variables to select a variable set that minimizes the Akaike Information Criterion (AIC) in the final model. At the end of the process, the final model exhibited lower AIC values compared with previously generated models and a Likelihood Ratio Test (LRT) was applied to test the difference between full and reduced models. Marginal and conditional  $R^2$  scores (Nakagawa & Schielzeth, 2013) were calculated to examine the variation explained by models using the "r.squaredGLMM" function in the "MuMIn" package. The variance inflation factor (VIF) was also computed with the "vif.mer" custom function to check for possible collinearity effects in the model.

Generalized Additive Models and LMM were performed for the entire period where growth and climatic data were both available at each study site (Table 1).

Finally, a Bayesian regression model (BRM), an independent method well suited for hierarchical data structures (Gelman & Hill, 2007), was employed to evaluate relationships between predictors and tree growth. The statistical model used in this analysis was analogous to a multiple regression with standardized (centered and scaled) variables. Our approach was hierarchical with a normally distributed random intercept and slope for each tree, assuming weak prior distributions (mean = 0 and standard deviation = 100) and a normal residual error distribution. Markov Chain Monte Carlo (MCMC) simulations were performed with the package "rstan" (version 2.16.2) running four different chains, each with 2000 "burn-in" and 8000 subsequent cycles with a thinning rate of 1 of 8 steps. The median, 2.5% and 97.5% quantiles were computed on the posterior distribution of regression coefficients and a significant

relationship was inferred if the interquartile interval did not overlap the zero value.

### 3 | RESULTS

Substantial variability in environmental conditions was detected among sites (Figure 1). Mean annual temperature ( $T$ ) and mean temperature during the growing period ( $T_g$ ) decreased with increased latitude (Figure 1a,c); atmospheric nitrogen deposition ( $N_{dep}$ ) also showed geographic variation, with increased  $N_{dep}$  at northern study sites 3 and 4 (close to industrialized area) (Figure 1e); annual precipitation did not show the same geographic pattern, with similar values between the southernmost site 1 and the northernmost site 4 (Figure 1b), however, a geographic pattern was observed for total precipitation during the growing period ( $P_g$ ) (Figure 1d); and SPEI showed similar average values at different sites (Figure 1f).

Long-term temporal variability in environmental variables (Figure S1) exhibited the following: (i) a steep increase in temperature at all sites in recent decades; (ii) a slight decrease in precipitation in

recent decades, more notable for site 3; (iii) more frequent negative “dry” values in recent decades at all sites, indicated by SPEI; and (iv) a steady increase in nitrogen deposition in recent decades, however, a tendency for  $N_{dep}$  to level off was observed, especially at northernmost sites 3 and 4.

The most relevant relationships observed were between the following environmental variables: (i) a negative correlation between precipitation during the growing period ( $P_g$ ) and temperature ( $T$  and  $T_g$ ,  $r = -0.68$ ,  $r = -0.65$ , respectively); (ii) a positive correlation between  $T$  and  $C_a$  ( $r = 0.41$ ); and (iii) with distinctive patterns at different study sites, a positive correlation between  $C_a$  and  $N_{dep}$  ( $r = 0.74$ ) (Figure S2).

Variability was observed in volume ( $G_V$ ) and height ( $G_H$ ) annual growth rates, within and among sites (Figure 2), with higher growth rates at southernmost site 1 (Figure 2). Statistical dependence was not observed between  $G_V$  and  $G_H$  when all data were pooled (Figure S3).

Evident patterns were observed in the relationship between cambial age (Age),  $G_V$ , and  $G_H$ . Results showed  $G_V$  increased steadily with Age and leveled off only when trees reached Age > 130 years,

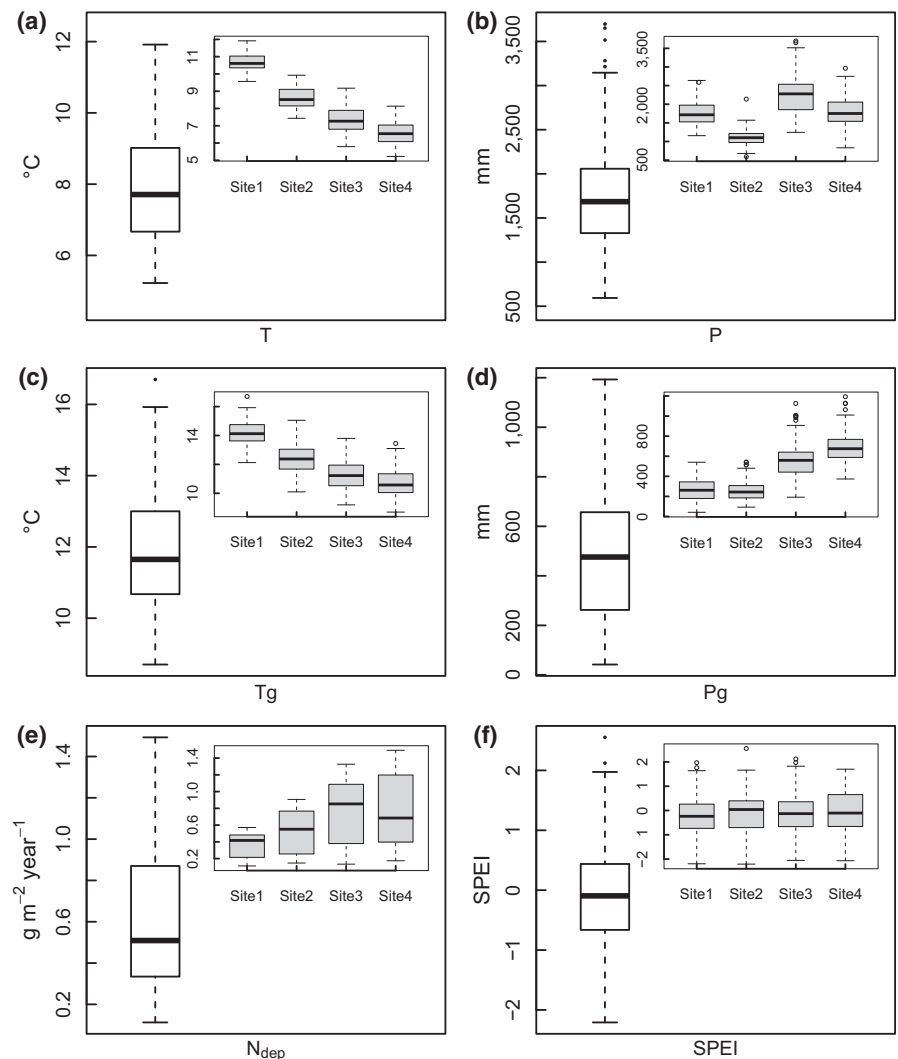


**FIGURE 1** Boxplots of explored long-term ranges of environmental variables, data of all sites pooled together;  $T$  = mean annual temperature;  $P$  = total annual precipitation;  $T_g$  = mean temperature during the growing period;  $P_g$  = total precipitation during the growing period;  $N_{dep}$  = annual rate of atmospheric nitrogen deposition; SPEI, standardized precipitation-evapotranspiration index. Each box represents the 75th to 25th percentiles, the bold line shows the median, upper and lower marks are the largest to smallest observation values which are less than or equal to the upper and lower quartiles plus 1.5 times the length of the interquartile range, Circles outside the lower upper mark range represent outliers. Inset graphs show the same values (with same notations) for the different studied sites (see Table 1)

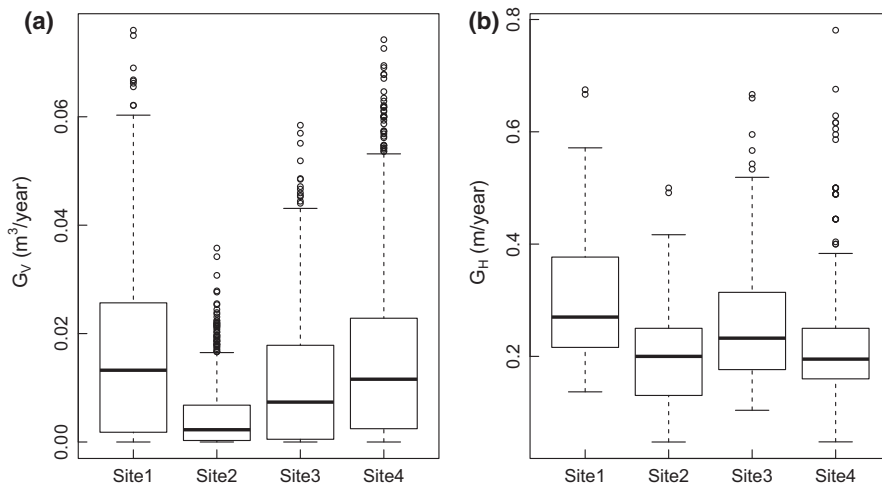


**FIGURE 2** Box plots of (panel a) stem volume annual growth ( $G_V$ ), and (panel b) stem height annual growth ( $G_H$ ) at the studied sites (see Table 1). Each box represents the 75th to 25th percentiles, the bold line shows the median, upper and lower marks are the largest to smallest observation values which are less than or equal to the upper and lower quartiles plus 1.5 times the length of the interquartile range. Circles outside the lower upper mark range represent outliers

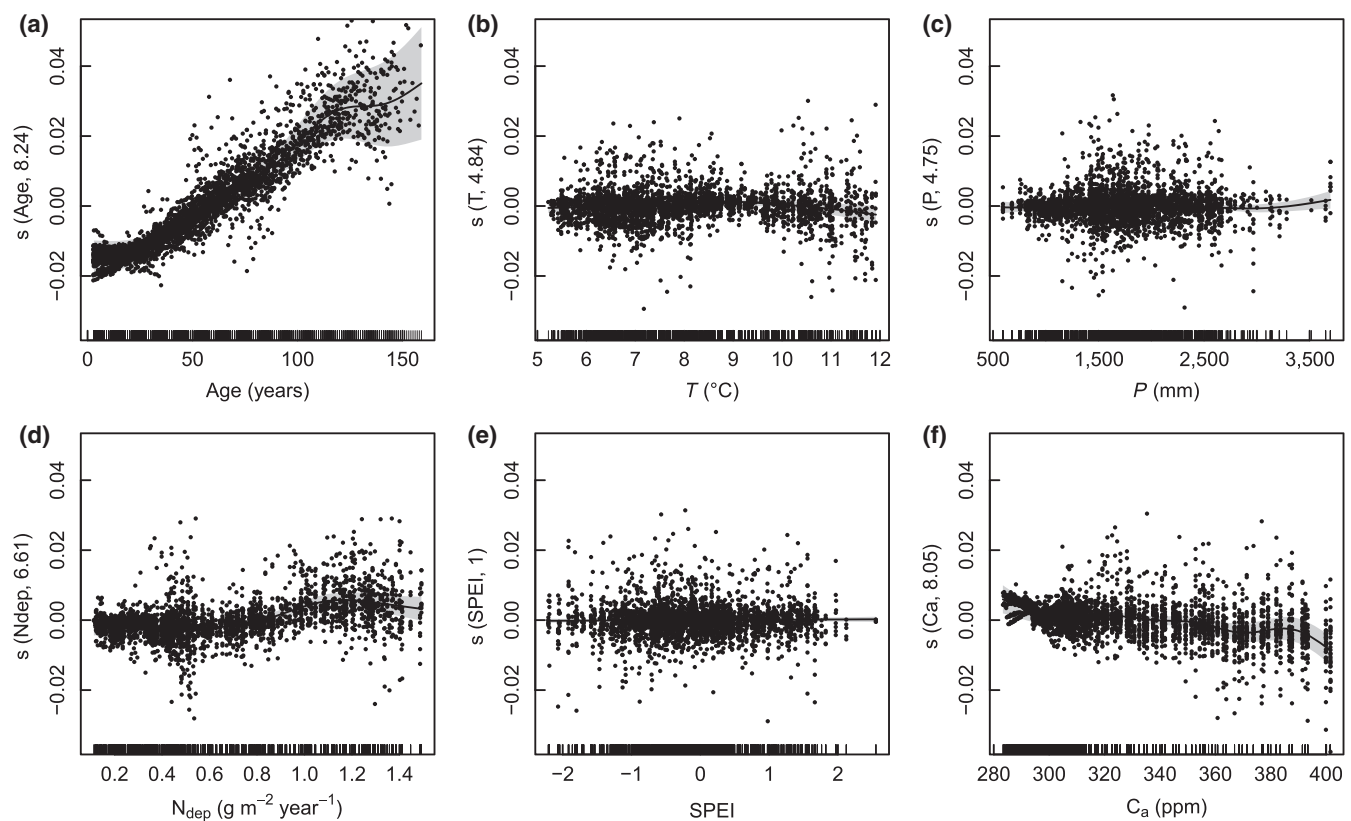


**FIGURE 3** Generalized Additive Model (GAM) results of environmental variables for stem volume annual growth ( $G_V$ ). Age = trees cambial age;  $T$  = mean annual temperature;  $P$  = total annual precipitation;  $N_{dep}$  = annual nitrogen deposition rate; SPEI, standardized precipitation-evapotranspiration index;  $C_a$  = atmospheric carbon dioxide concentration. The y-axis values indicate x-axis covariate effects on deviation from the mean predicted by the model (continuous line). The shaded areas indicate the 95% confidence interval. The number on each y-axis caption is the effective degrees of freedom for the term plotted. The small lines along the x-axis are the “rug”, which show the observation density. The continuous line is an estimate of the smooth function of the partial residuals (thus, the y-axis is centered on zero) and indicates the x-axis covariate effects on the measured trait. In these plots, a positive slope of the continuous line shows a positive effect of the x-variable, and a negative slope of the line indicates a negative effect

approximately;  $G_H$  increased steeply with Age, however,  $G_H$  peaked quite early (aged 30 years, approximately) and subsequently steadily decreased (Figure S4, but see also GAM results below).

Generalized Additive Models (GAM) were applied to the entire dataset (data from all sites pooled) to describe predictor variable effects (independent of each other) on  $G_V$  and  $G_H$  of a given  $t$  year.

We used the following as predictor variables: cambial age (Age), mean annual temperature ( $T$ ), total annual precipitation ( $P$ ) [or alternatively, growing period mean temperature and total precipitation,  $T_g$  and  $P_{g,l}$ ], mean annual N deposition ( $N_{dep}$ ) rate, atmospheric  $CO_2$  concentration ( $C_a$ ), and SPEI index. GAM plots (Figures 3a and 4a) confirmed the strong Age effect on  $G_V$  and  $G_H$ , with patterns similar

to those shown in Figure S4 and results described above. GAM results indicated environmental variables exhibited a weak effect on  $G_V$  (Figure 3b,c,e,f), with the exception of an apparent positive  $N_{dep}$  response at low  $N_{dep}$  values (Figure 3d). A slightly positive  $G_H$  trend was observed in  $T$  (Figure 4b) and a more pronounced positive trend in  $N_{dep}$ , up to values of approximately  $1 \text{ g m}^{-2} \text{ y}^{-1}$  (Figure 4d). An association with SPEI was not apparent (Figure 4f) and if we consider GAM plots in regions of highest observation densities (i.e. x-axis portions with “thickened” lines), patterns were also not associated with  $P$  (Figure 4c) and a slight positive trend was detected with  $C_a$  (Figure 4e). When  $T_g$  and  $P_g$  were replaced as covariates for annual  $T$  and  $P$  values, appreciable differences in  $G_V$  were not detected. A  $G_H$  relationship with temperature was not observed when  $T_g$  and  $P_g$  were applied as covariates, however, the positive  $N_{dep}$  response remained notable (Figures S5 and S6).

Generalized Additive Models analysis for  $N_{dep}$  effects on  $G_H$  was repeated separately for each study site using the same set of covariates. Results revealed positive  $N_{dep}$  effects on  $G_H$  at low  $N_{dep}$  values ( $N_{dep} < 1 \text{ g m}^{-2} \text{ y}^{-1}$ ), whereas a threshold effect was suggested at sites with higher N loads (sites 3 and 4) for  $N_{dep}$  values

$> 1 \text{ g m}^{-2} \text{ y}^{-1}$  (Figure 5). GAM statistics are shown in Tables S3, S4, and S5 of Supporting Information.

A linear mixed-effect model (LMM) was chosen to describe variation in  $G_V$  and  $G_H$ , including all covariates (Age,  $T$  (and  $T_g$ ),  $P$  (and  $P_g$ ),  $N_{dep}$ ,  $C_a$ , and SPEI); previous year's mean annual temperature ( $T_{t-1}$ ) and total annual precipitation ( $P_{t-1}$ ) were also included. Following the procedure described in the methods, we initiated the analysis by simplifying a rather complex model, including variable-covariate interactions. Indeed, AIC scores suggested including interaction terms slightly increased the model's predictive capacity. Model structures, covariates with model coefficients, standard errors, and significance levels are summarized in Table 2 for  $G_V$ , and Table 3 for  $G_H$ . Model results explained a suitable proportion of total variability, higher for  $G_V$  (approximately 85%) than  $G_H$  (approximately 60%). A rather large proportion of total variance was explained by trees within sites, as shown by intraclass correlation coefficients (ICC).

Analysis of a single covariate effect indicated a significant effect in Age and  $N_{dep}$  for all cases and the following specific results: (i) for Age, a significant effect was present in  $G_V$  and  $G_H$  for all tested models; a significant positive effect for  $G_V$ , and a negative effect for

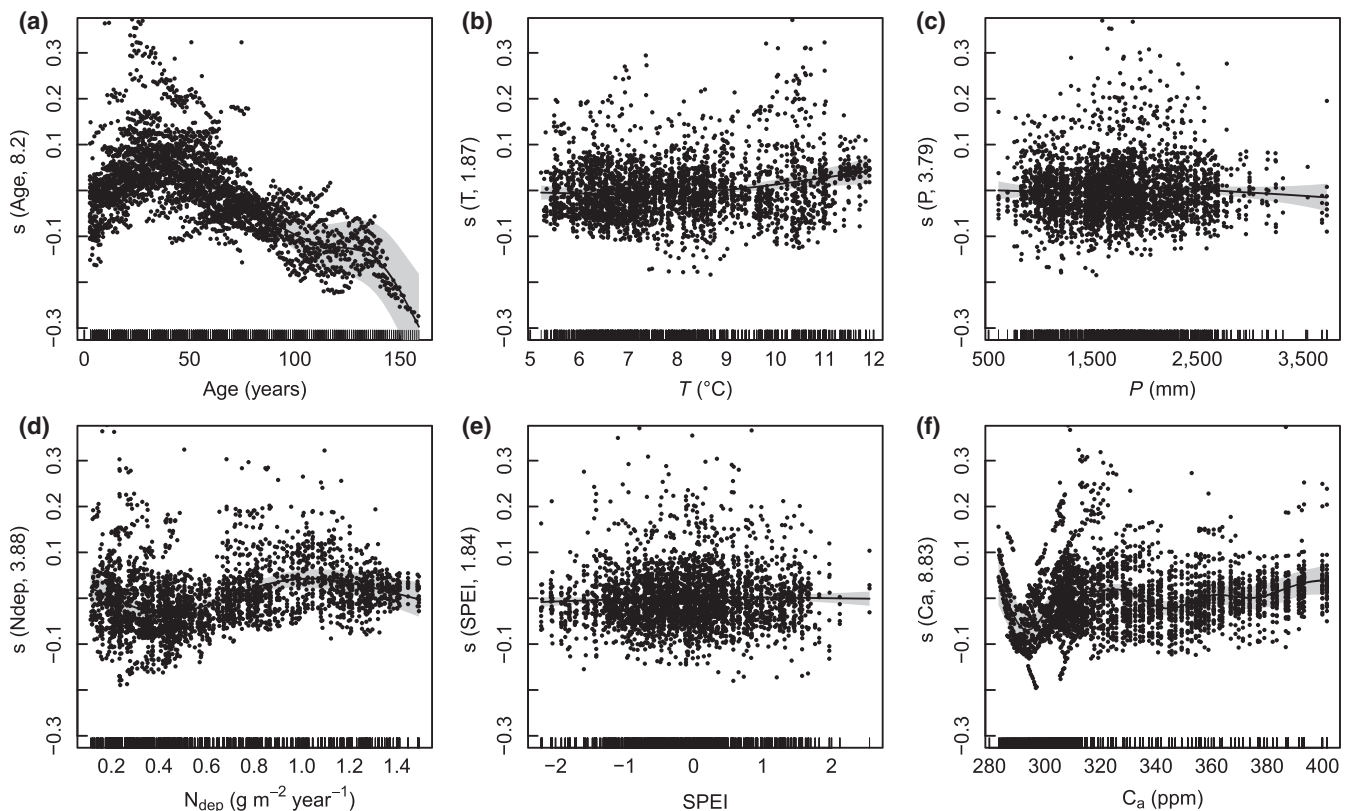


**FIGURE 4** Generalized Additive Model (GAM) results of environmental variables for stem height annual growth ( $G_H$ ). Age = trees cambial age;  $T$  = mean annual temperature;  $P$  = total annual precipitation;  $N_{dep}$  = annual nitrogen deposition rate; SPEI, standardized precipitation-evapotranspiration index;  $C_a$  = atmospheric carbon dioxide concentration. The y-axis values indicate x-axis covariate effects on deviation from the mean predicted by the model (continuous line). The shaded areas indicate the 95% confidence interval. The number on each y-axis caption is the effective degrees of freedom for the term plotted. The small lines along the x-axis are the “rug”, which show the observation density. The continuous line is an estimate of the smooth function of the partial residuals (thus, the y-axis is centered on zero) and indicates the x-axis covariate effects on the measured trait. In these plots, a positive slope of the continuous line shows a positive effect of the x-variable, and a negative slope of the line indicates a negative effect

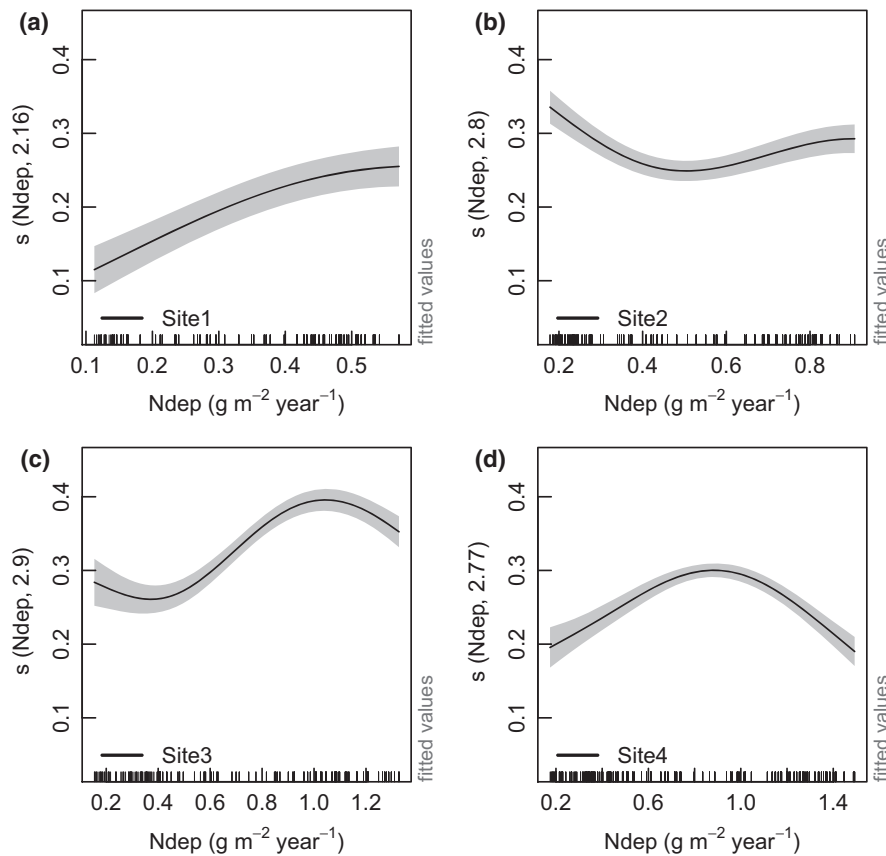


**FIGURE 5** Generalized Additive Model (GAM) results of nitrogen deposition  $N_{\text{dep}}$  for stem height annual growth ( $G_{\text{H}}$ ) at different sites (panel a: site1; panel b: site2; panel c: site3; panel d: site4); cambial age, mean annual temperature, total annual precipitation, standardized precipitation–evapotranspiration index, atmospheric carbon dioxide concentration, mean annual temperature of the previous year and total precipitation of the previous year were also included in the model as covariates. The y-axis values indicate x-axis covariate effects on deviation from the mean predicted by the model (continuous line). The shaded areas indicate the 95% confidence interval. The number on each y-axis caption is the effective degrees of freedom for the term plotted. The small lines along the x-axis are the “rug,” which show the observation density. The continuous line is an estimate of the smooth function and indicates the x-axis covariate effects on the measured trait. In these plots, a positive slope of the continuous line shows a positive effect of the x-variable, and a negative slope of the line indicates a negative effect

$G_{\text{H}}$ ; (ii) for  $N_{\text{dep}}$  a significant, positive effect was detected for  $G_{\text{V}}$  and  $G_{\text{H}}$  in full and reduced models; and (iii) for  $C_{\text{a}}$  a significant positive effect was shown for  $G_{\text{H}}$  in the reduced model.

Interactions between some environmental variables showed significant effects in  $G_{\text{V}}$  for the full and reduced model:  $T \times N_{\text{dep}}$  (negative),  $T \times C_{\text{a}}$  (positive),  $\text{SPEI} \times N_{\text{dep}}$  (negative),  $\text{SPEI} \times C_{\text{a}}$  (positive), and  $N_{\text{dep}} \times C_{\text{a}}$  (negative). A significant negative effect in the full and reduced model was indicated in  $G_{\text{H}}$  only for the  $N_{\text{dep}} \times C_{\text{a}}$  interaction.

Linear mixed-effects models analysis was repeated using growing season temperature ( $T_{\text{g}}$ ) and precipitation ( $P_{\text{g}}$ ), instead of mean annual temperature and total annual precipitation. The only difference in results of single covariate effects was in the reduced model as follows: a significant positive effect of  $C_{\text{a}}$  on  $G_{\text{V}}$  and  $G_{\text{H}}$  and a significant positive effect of SPEI on  $G_{\text{H}}$  (Tables S6 and S7 in Supporting Information).

We acknowledged a potential collinearity problem might affect our LMM analyses, because results revealed specific variable correlation in the dataset, i.e.  $N_{\text{dep}}$  and  $C_{\text{a}}$  (Figure S2). This correlation might influence the individual predictor coefficients and

determination, therefore producing the response variable effect might be challenging. Overall, variance inflation factors (VIFs) and kappa number calculations showed collinearity was a concern only for some interactive terms in full LMM models, however, no major threat from collinearity was apparent in LMM reduced models (Table S8).

Bayesian regression model (BRM) for single covariate effects (Figure 6) confirmed significant and positive effects of Age and  $N_{\text{dep}}$  in  $G_{\text{V}}$  and a significant and positive effect of  $N_{\text{dep}}$  in  $G_{\text{H}}$ , as observed in LMM models; and the negative relationship between  $G_{\text{V}}$  and  $C_{\text{a}}$ , as observed in GAM. It must be noted BRM showed no significant effects of climatic drivers ( $T$ ,  $P$ , and SPEI) on  $G_{\text{V}}$  and  $G_{\text{H}}$  (Figure 6), consistent with the weak effect observed in LMM and GAM.

## 4 | DISCUSSION

Our study investigated long-term variability in growth rates (stem volume and stem height) of dominant beech (*F. sylvatica*) trees along a geographic transect and examined explanatory variables among



**TABLE 2** Linear mixed-effect models. Fit of stem volume growth ( $G_V$ ) as a function of site-specific environmental variables. Cf: standardized coefficients of predictor variables;  $I$  = confidence interval. Age = tree cambial age;  $T$  = mean annual temperature;  $P$  = total annual precipitation; SPEI = standardized precipitation-evapotranspiration index;  $N_{\text{dep}}$  = annual rate of nitrogen deposition;  $C_a$ : atmospheric  $\text{CO}_2$  concentration;  $T_{t-1}$  = previous year mean annual temperature;  $P_{t-1}$  = previous year total annual precipitation; ICC = Intraclass Correlation; Obs: number of observations;  $R_m^2$  = marginal R-square (proportion of variance explained by fixed factors);  $R_c^2$  = conditional R-square (proportion of variance explained by fixed and random factors); AIC = Akaike Information Criterion; BIC = Bayesian Information Criterion. \*, \*\* and \*\*\* denote statistical significance at  $p < .05$ ,  $p < .01$  and  $p < .001$ , respectively

	Full model		Reduced model	
	Cf	$I$	Cf	$I$
Age	0.375***	(0.282 to 0.468)	0.371***	(0.280 to 0.462)
$P$	-0.002	(-0.030 to 0.027)		
$T$	0.022	(-0.029 to 0.073)	0.023	(-0.026 to 0.073)
SPEI	-0.010	(-0.038 to 0.018)	-0.009	(-0.026 to 0.008)
$N_{\text{dep}}$	0.370***	(0.303 to 0.436)	0.388***	(0.325 to 0.451)
$C_a$	0.109	(-0.042 to 0.260)	0.095	(-0.054 to 0.244)
$T_{(t-1)}$	-0.007	(-0.059 to 0.044)		
$P_{(t-1)}$	0.007	(-0.023 to 0.037)		
$T_{(t-1)} \times P_{(t-1)}$	0.005	(-0.022 to 0.031)		
$P \times T$	0.047**	(0.011 to 0.083)		
$P \times \text{SPEI}$	-0.007	(-0.023 to 0.009)		
$P \times N_{\text{dep}}$	0.038	(-0.007 to 0.083)		
$P \times C_a$	-0.039	(-0.088 to 0.009)		
$T \times \text{SPEI}$	-0.028	(-0.063 to 0.007)		
$T \times N_{\text{dep}}$	-0.097***	(-0.144 to -0.050)	-0.094***	(-0.139 to -0.048)
$T \times C_a$	0.085**	(0.033 to 0.137)	0.088**	(0.037 to 0.140)
$\text{SPEI} \times N_{\text{dep}}$	-0.090***	(-0.138 to -0.043)	-0.070**	(-0.096 to -0.045)
$\text{SPEI} \times C_a$	0.076**	(0.024 to 0.127)	0.053**	(0.029 to 0.078)
$N_{\text{dep}} \times C_a$	-0.128***	(-0.183 to -0.072)	-0.128***	(-0.182 to -0.074)
ICC	0.696		0.699	
Obs	3065		3065	
$R_m^2$	0.516		0.512	
$R_c^2$	0.854		0.855	
AIC	3202.90		3194.00	
BIC	3353.60		3290.45	

ontogenetic (tree age) and environmental drivers (climatic factors and atmospheric nitrogen deposition).

#### 4.1 | Age-dependent dynamics and climatic effects

Tree age was the main explanatory variable for tree growth variability, however, age-dependent dynamics differed between stem and height growth. Cienciala et al. (2016) reported similar results on the key role of tree age/size on shaping forest productivity. Stem growth increased steadily, consistent with tree age, until approximately 130 years, and growth tended to stabilize (but not decline) thereafter. Therefore, age-related constraints (Ryan, Binkley, & Fownes, 1997) were not visible for single trees. Instead, an age-related decline was apparent for height growth: following an initial increase and early ontogenetic peak at approximately 30 years of age, a downtrend was indeed evident; however, growth did not fall below

a maximum 50% growth rate and remained approximately constant until trees exceeded 100 years of age.

These patterns might be interpreted at the following two levels: (i) at the individual dominant tree level; and (ii) at the population level. The steady increased tree growth with age, which implies increased tree dimension, was consistent with Stephenson et al. (2014) in a number of tree species, where results showed even large and old trees continued to take up large carbon amounts, possibly by increasing individual leaf area and reducing competition during stand development. Age dynamics in height growth might be better explained at population levels, with the assumption that dominant (upper canopy) height is a viable proxy for aboveground productivity, the so-called Eichhorn's rule (Eichhorn, 1904); but also see Assmann (1970) and Skovsgaard and Vanclay (2008). In so doing, our results suggested age-related constraints on stand productivity were effective rather early in beech forests, as shown by De Simon, Alberti,

**TABLE 3** Linear mixed-effect models. Fit of stem height growth ( $G_{t+1}$ ) as a function of site-specific environmental variables. Cf: standardized coefficients of predictor variables;  $I$  = confidence interval. Age: = tree cambial age;  $T$  = mean annual temperature;  $P$  = total annual precipitation; SPEI = standardized precipitation-evapotranspiration index;  $N_{\text{dep}}$  = annual rate of nitrogen deposition;  $C_a$ : atmospheric  $\text{CO}_2$  concentration;  $T_{t-1}$  = previous year mean annual temperature;  $P_{t-1}$  = previous year total annual precipitation; ICC = Intraclass Correlation; Obs: number of observations;  $R_m^2$  = marginal R-square (proportion of variance explained by fixed factors);  $R_c^2$  = conditional R-square (proportion of variance explained by fixed and random factors); AIC = Akaike Information Criterion; BIC = Bayesian Information Criterion. \*, \*\* and \*\*\* denote statistical significance at  $p < .05$ ,  $p < .01$  and  $p < .001$ , respectively

	Full model		Reduced model	
	Cf	$I$	Cf	$I$
Age	-0.397***	(-0.516 to -0.277)	-0.423***	(-0.545 to -0.301)
$P$	0.041	(-0.009 to 0.090)	0.024	(-0.021 to 0.069)
$T$	0.025	(-0.065 to 0.114)	0.033	(-0.053 to 0.118)
SPEI	-0.007	(-0.055 to 0.042)	0.024	(-0.012 to 0.061)
$N_{\text{dep}}$	0.172**	(0.059 to 0.285)	0.161**	(0.059 to 0.262)
$C_a$	0.142	(-0.100 to 0.384)	0.224*	(0.002 to 0.447)
$T_{(t-1)}$	0.040	(-0.047 to 0.127)		
$P_{(t-1)}$	0.050	(-0.002 to 0.102)		
$T_{(t-1)} \times P_{(t-1)}$	-0.034	(-0.081 to 0.013)		
$P \times T$	-0.034	(-0.098 to 0.030)	-0.055**	(-0.099 to -0.016)
$P \times \text{SPEI}$	-0.025	(-0.054 to 0.004)		
$P \times N_{\text{dep}}$	0.032	(-0.048 to 0.113)		
$P \times C_a$	-0.006	(-0.092 to 0.080)		
$T \times \text{SPEI}$	-0.046	(-0.108 to 0.016)		
$T \times N_{\text{dep}}$	-0.085*	(-0.156 to -0.005)		
$T \times C_a$	0.086	(-0.006 to 0.179)		
$\text{SPEI} \times N_{\text{dep}}$	-0.039	(-0.123 to 0.046)		
$\text{SPEI} \times C_a$	0.084	(-0.007 to 0.176)	0.040**	(0.011 - 0.070)
$N_{\text{dep}} \times C_a$	-0.204***	(-0.278 to -0.129)	-0.229***	(-0.298 to -0.160)
ICC	0.555		0.568	
Obs	3065		3065	
$R_m^2$	0.126		0.118	
$R_c^2$	0.606		0.614	
AIC	6718.69		6711.91	
BIC	6875.41		6817.06	

Delle Vedove, Zerbi, and Peressotti (2012). On the other hand, aboveground productivity was suggested to remain positive until late developmental stages, consistent with the long-term net primary productivity patterns observed by Xu et al. (2012).

The effects of climatic variables on tree growth were estimated in GAM, LMM, and BRM models. Across the considered geographic range, trees at the study sites grow in the cool-humid belt of Italian mountains; under these conditions, results indicated stem volume growth was largely free from climatic drivers (mean annual temperature  $T$  and mean  $T_g$ , total annual precipitation  $P$  and  $P_g$  during the growing period) and unaffected by increased atmospheric  $\text{CO}_2$ . Similarly, stem height growth was weakly affected by climatic variables, however, a slight positive temperature effect was apparent in GAM results.

This weak observed dependence of tree growth on climatic variables appeared rather at odds with the general hypothesis that

anthropogenic climate change is an important driver of forest productivity levels via the fertilization effect of enhanced atmospheric  $\text{CO}_2$ . Furthermore, indirect effects, including increased temperatures and modified precipitation patterns were expected to influence productivity (Giammarchi, Cherubini, Pretzsch, & Tonon, 2017, IPCC 2014).

Clear relationships between radial (or basal area) growth rates and climatic variables were in fact not present in long-term tree ring studies across a number of forest tree species (e.g. Borghetti, Gentilesca, Leonardi, van Noije, & Rita, 2017; Peñuelas, Canadell, & Ogaya, 2011). Furthermore, in recent synchronic studies based on forest inventory plot analyses (Cienciala et al., 2016), the footprint from environmental and climatic drivers on tree growth was found weaker than size/age and competition effects and above ground biomass did not have a direct relationship to rainfall and temperature in tropical forests across altitudinal gradients (Venter et al., 2017). In

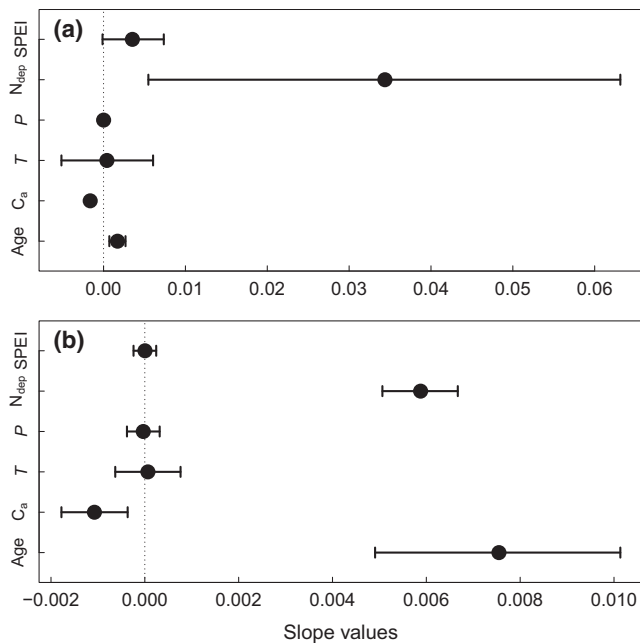


**FIGURE 6** Results of the Bayesian regression model. Circles are median values for slopes of relationships between considered drivers on the y-axis (Age = tree cambial age;  $C_a$  = atmospheric  $\text{CO}_2$  concentration;  $T$  = mean annual temperature;  $P$  = total annual precipitation;  $N_{\text{dep}}$  = annual rate of nitrogen deposition; SPEI, standardized precipitation-evapotranspiration index) and stem annual volume growth ( $G_v$ , upper panel) and stem annual height growth ( $G_H$ , lower panel). Positive and negative values indicate positive and negative effects, respectively. Bars represent the 95% confidence interval, if overlapping the zero line slopes were not significant

several cases, studies demonstrated environmental changes could offset each other. For example, under an unfavorable temperature and precipitation balance, stress conditions could override the beneficial effects of increasing atmospheric  $\text{CO}_2$  (Groenendijk et al., 2015; Silva & Anand, 2013; Zang, Hartl-Meier, Dittmar, Rothe, & Menzel, 2014).

Poor relationships between growth and climatic variables confirmed tree growth rates could be poor climatic proxies under rapidly changing environmental conditions (Briffa et al., 1998); and suggested trees exhibit potential to adjust to climatic variability and maintain functional homeostasis (e.g. Magnani, Grace, & Borghetti, 2002). Borghetti et al. (2017) reported acclimation to changing environmental conditions might result from coordination of several complementary traits and increased nitrogen availability due to N deposition might be an additional resource trees use to achieve functional acclimation.

Some studies, however, point in a different direction and suggest climatic variability effects on forest productivity. For example, Latte, Perin, Kint, Lebourgeois, and Claessens (2016) showed major growth rate changes in beech forests of Central Europe were related to climate change; in particular Härdtle et al. (2013) in Luxembourg, and Knutzen, Dulamsuren, Meier, and Leusche (2017) in Central Germany found precipitation to be an important predictor of radial increments, and Dulamsuren, Hauck, Kopp, Ruff, and

Leuschner (2017) in south-western Germany identified moisture and temperature as limiting factors on radial growth. However, Aertsens et al. (2014) reported negative environmental effects on growth changes were buffered in highly productive sites; drought-driven growth reductions were detected in beech on the Mediterranean mountains (Jump et al., 2006; Piovesan et al., 2008), however, these effects were mainly observed in old forests, where climate sensitivity might be greater (Carrer & Urbinati, 2004; Esper, Niederer, Bebi, & Frank, 2008). Other studies in beech forests (Tegel et al., 2014) did not detect an effect of increasing drought on tree growth in southern Europe, and recently, Cavin and Jump (2017) proposed the hypothesis that lower sensitivity to drought in dry range edge populations might be driven primarily by local climatic factors. In our study, the more evident response to climatic variables was a positive height growth to mean annual temperature response (but not to mean growing period temperature). In addition to a direct biological affect, this might also suggest an effect due to an extension of the growing season (Menzel & Fabian, 1999; Pretzsch et al., 2014).

## 4.2 | The role of nitrogen deposition

First, we recognized a potential uncertainty influencing our results in the link between  $N_{\text{dep}}$  and tree growth; indeed,  $N_{\text{dep}}$  rates in our study were modeled data, with a  $1.9 \times 2^\circ$  resolution, therefore grid values could diverge from actual conditions where trees were growing. These divergence effects can hardly be estimated, however, we might expect some level of additional introduced variability, with the subsequent possibility of weakened relationships between  $N_{\text{dep}}$  and tree growth rates.

In analyses performed (GAM, LMM, and RGM), a positive  $N_{\text{dep}}$  effect on height ( $G_H$ ) and volume ( $G_v$ ) growth was apparent. As discussed earlier, the positive  $G_H$  effects can be interpreted as positive  $N_{\text{dep}}$  effects on aboveground stand productivity; similarly, maximum growth rate variation in dominant height was interpreted as variation in stand productivity due to regional differences in N loads (Bontempis et al., 2011).

The positive  $N_{\text{dep}}$  effects appeared to stabilize at values exceeding approximately  $1.0 \text{ g m}^{-2} \text{ y}^{-1}$ , supporting the hypothesis that a threshold load exists, where forest ecosystems do not respond to additional N (Aber et al., 1998). The observed negative  $N_{\text{dep}} \times C_a$  interaction (Tables 2 and 3) might be the consequence of study sites reaching  $N_{\text{dep}}$  threshold effects in recent years, during which a constant rise of  $C_a$  was reported. At the global level, Leonardi et al. (2015) reported mean N deposition rates for deciduous broad-leaf and mixed forests were  $0.6\text{--}0.7 \text{ g m}^{-2} \text{ y}^{-1}$ , with large areas below  $0.1 \text{ g m}^{-2} \text{ y}^{-1}$ . Therefore, over the next few decades, unintended soil N fertilization associated with  $N_{\text{dep}}$  might have an effect on forest productivity over large forest areas. However, Hyvönen et al. (2007) suggested the magnitude and persistence of the response largely depends on the underlying biological mechanisms and the short- or long-term effects.

We largely reconciled our results with previous findings on the effects of increased nitrogen supplies on forest ecosystems (e.g. de

Vries et al., 2014). Nonetheless, our results were the first to include annual  $N_{\text{dep}}$  rates as a driver of long-term forest growth and provided a long-term perspective to studies in which the effects of nitrogen availability on stand growth and carbon uptake were experimentally explored over shorter time periods (e.g. Ferretti et al., 2014; From, Lundmark, Morling, Pommerening, & Nordin, 2016; Gentilescia et al., 2013; de Vries et al., 2009) or were compared by synchronic approaches among inventory plots characterized by different nutritional status (e.g. Solberg et al., 2009, Cienciala et al., 2016).

We agree N deposition effects can vary as a result of the nature and chemical characteristics of the soil, in particular the same N deposition load can drive a different effect if a critical threshold is reached under different soil conditions. For instance, a decline in C/N due to N deposition can stimulate N mineralization and N plant uptake, coincident with nitrification and N leaching if a saturation threshold is overcome (Aber et al., 1998); indeed, Gentilescia et al. (2013) showed  $N_{\text{dep}}$  effects on tree and stand growth varied as a consequence of differences in site-specific accumulated nitrogen deposition and soil fertility. It is noteworthy, however, that response curves for our individually analyzed sites (Figure 5) showed a rather consistent positive  $G_H$  to  $N_{\text{dep}}$  response for values  $<1.0 \text{ g m}^{-2} \text{ y}^{-1}$ . This might suggest site-related effects can be bypassed due to deposited nitrogen utilization by direct canopy uptake (Sparks, 2009). Estimates of N retention by canopies strongly varied, but were reported up to 70% (Dail et al., 2009; Gaige et al., 2007; Sievering, Tomaszewski, & Torizzo, 2007). Recent studies confirmed an active role of tree canopies in  $N_{\text{dep}}$  processing and N uptake (Guerrieri, Vanguelova, Michalski, Heaton, & Mencuccini, 2015; Guerrieri et al., 2011; Zhang et al., 2015). These results might explain short-term effects on tree growth (Dail et al., 2009; Pregitzer, Burton, Zak, & Talhelm, 2008) and positive relationships between  $N_{\text{dep}}$  and functional traits, including plant water-use efficiency (Leonardi et al., 2012).

However, increased long-term  $N_{\text{dep}}$  effects cannot be ruled out. The effects might be mediated by declines in the C/N ratio in soil organic matter, which can stimulate mineralization and plant N uptake (Aber et al., 2003) or by plant acclimation processes, including changes in xylem functional anatomy and conduction efficiency (Borghetti et al., 2017). Among long-term consequences, the implications of height growth stimulation cannot be disregarded, as it affects tree capacity to compete in mixed forests, with potential effects on community species composition (Bontemps, Hervé, Duplat, & Dhôte, 2012).

Overall, the following conclusions can be drawn from this study: (i) we found limited evidence of recent climatic variability effects on annual growth rates of canopy beech trees sampled across a geographic gradient in the montane belt of the Italian peninsula; and (ii) among environmental drivers, nitrogen deposition exhibited the most evident role, with a significant effect on volume and height growth rates; the positive effect on canopy height growth rate can be interpreted as a positive effect on above-ground net productivity of the selected beech forests. A large proportion of temperate forests are currently growing in areas where nitrogen deposition is below the

value at which the positive effects on forest growth appeared to level off in our study (approximately  $1 \text{ g m}^{-2} \text{ y}^{-1}$ ), therefore unintended fertilization due anthropogenic global change should be monitored in evaluations of long-term forest productivity dynamics.

## ACKNOWLEDGEMENTS

The research was supported by the MIUR-PRIN Grant No. 2012E3F3LK "Global change effects on the productivity and radiative forcing of Italian forests: a novel retrospective, experimental and prognostic analysis." For helpful support in field work, we sincerely thank: M. Basile, R. Bicchocchi, E. Frassinetti, G. Gori, A. Lapolla, S. Milito, R. Pettinà, A. Poletto, and G. Ventura. For technical support and useful discussion, we also thank M. Bascietto, N. Moretti, F. Ripullone and L. Todaro. As for CMIP6 nitrogen deposition data we used in our analyses, we acknowledge the World Climate Research Programme which, through its Working Group on Coupled Modelling, coordinated and promoted CMIP6; in particular, we thank the climate modeling groups for producing and making available their model output, the Earth System Grid Federation (ESGF) for archiving the data and providing access, and the multiple funding agencies who support CMIP6 and ESGF. The comments of three anonymous reviewers and the suggestions by the subject editor contributed to improve the manuscript.

## ORCID

Marco Borghetti  <http://orcid.org/0000-0003-3159-6655>

## REFERENCES

- Aber, J. D., Goodale, C. L., Ollinger, S. V., Smith, M.-L., Magill, A. H., Martin, M. E., ... Stoddard, J. L. (2003). Is nitrogen deposition altering the nitrogen status of northeastern forests? *BioScience*, 53, 375–389.
- Aber, J. D., McDowell, W., & Nadelhoffer, K. J. (1998). Nitrogen saturation in temperate forest ecosystems. *BioScience*, 48, 921–34.
- Aertsen, W., Janssen, E., Kint, V., Bontemps, J.-D., Orshoven, J. V., & Muys, B. (2014). Long-term growth changes of common beech (*Fagus sylvatica* L.) are less pronounced on highly productive sites. *Forest Ecology and Management*, 312, 252–259.
- Assmann, E. (1970). *The Principles of Forest Yield Study*. Oxford: Pergamon Press pp. 45, 160–163.
- Bascietto, M., Cherubini, P., & Scarascia Mugnozza, G. (2004). Tree rings from a European beech forest chronosequence are useful for detecting growth trends and carbon sequestration. *Canadian Journal of Forest Research*, 34, 481–492.
- Beguéría, S., & Vicente-Serrano, S.M. (2013). SPEI: Calculation of the Standardised Precipitation-Evapotranspiration Index. R package version 1.6. <https://CRAN.R-project.org/package=SPEI>
- Boisvenue, C., & Running, S. W. (2006). Impacts of climate change on natural forest productivity – evidence since the middle of the 20th century. *Global Change Biology*, 12, 862–882.
- Bontemps, J. D., Hervé, J. C., & Dhôte, J. F. (2009). Long-term changes in forest productivity: a consistent assessment in even-aged stands. *Forest Science*, 55, 549–564.
- Bontemps, J. D., Hervé, J. C., & Dhôte, J. F. (2010). Dominant radial and height growth reveal comparable historical variations for common

- beech in north-eastern France. *Forest Ecology and Management*, 259, 1455–1463.
- Bontemps, J. D., Hervé, J. C., Duplat, P., & Dhôte, J. F. (2012). Shifts in the height-related competitiveness of tree species following recent climate warming and implications for tree community composition: the case of common beech and sessile oak as predominant broad-leaved species in Europe. *Oikos*, 121, 1287–1299.
- Bontemps, J. D., Hervé, J. C., Leban, J. M., & Dhôte, J. F. (2011). Nitrogen footprint in a long-term observation of forest growth over the twentieth century. *Trees-Structure and Function*, 25, 237–251.
- Borghetti, M., Gentilescà, T., Leonardi, S., van Noije, T., & Rita, A. (2017). Long-term temporal relationships between environmental conditions and xylem functional traits: a meta-analysis across a range of woody species along climatic and nitrogen deposition gradients. *Tree Physiology*, 37, 4–17.
- Briffa, K. R., Schweingruber, F. H., Jones, P. D., Osborn, T. J., Harris, I. C., Shiyatov, S. G., ... Grudd, A. H. (1998). Trees tell of past climates: but are they speaking less clearly today? *Philosophical Transaction Royal Society London B*, 353, 65–73.
- Brunetti, M., Lentini, G., Maugeri, M., Nanni, T., Simolo, C., & Spinoni, J. (2012). Projecting North Eastern Italy temperature and precipitation secular records onto a high resolution grid. *Physics and Chemistry of the Earth*, 40–41, 9–22.
- Brunetti, M., Maugeri, M., Nanni, T., Simolo, C., & Spinoni, J. (2014). High-resolution temperature climatology for Italy: interpolation method intercomparison. *International Journal of Climatology*, 34, 1278–1296.
- Burnham, K. P., & Anderson, D. R. (2002). *Model Selection and Multimodel Inference: A Practical Information-Theoretic Approach*. New York, NY: Springer Science+Business Media Inc.
- Carrer, M., & Urbinati, C. (2004). Age-dependent tree-ring growth responses to climate in *Larix decidua* and *Pinus cembra*. *Ecology*, 85, 730–740.
- Cavin, L., & Jump, A. S. (2017). Highest drought sensitivity and lowest resistance to growth suppression are found in the range core of the tree *Fagus sylvatica* L. not the equatorial range edge. *Global Change Biology*, 23, 362–379.
- Churkina, G., Zaehle, S., Hughes, J., Viovy, N., Chen, Y., Jung, M., ... Jones, C. (2010). Interactions between nitrogen deposition, land cover conversion, and climate change determine the contemporary carbon balance of Europe. *Biogeoscience*, 7, 2749–2764.
- Ciais, P., Schelhaas, M. J., Zaehle, S., Piao, S. L., Cescatti, A., Liski, J., ... Nabuurs, G. J. (2008). Carbon accumulation in European forests. *Nature Geoscience*, 1, 425–429.
- Cienciala, E., Russ, R., Santruckova, H., Altman, J., Kopáček, J., Hünová, I., ... Stáhl, G. (2016). Discerning environmental factors affecting current tree growth in Central Europe. *Science of the Total Environment*, 573, 541–554.
- Cook, E.R., Krusic, P.J., Holmes, R.H., & Peters, K. (2007). Program ARSTAN Ver. 41d. Available at [www.ldeo.columbia.edu/tree-ring-lab/oratory](http://www.ldeo.columbia.edu/tree-ring-lab/oratory).
- Crespi, A., Brunetti, M., Lentini, G., & Maugeri, M. (2018). 1961–1990 high-resolution monthly precipitation climatologies for Italy. *International Journal of Climatology*, 38, 878–895.
- Dail, D. B., Hollinger, D. Y., Davidson, E. A., Fernandez, I., Sievering, H. C., Scott, N. A., & Gaige, E. (2009). Distribution of nitrogen 15-tracers applied to the canopy of a mature spruce-hemlock stand, Howland, Maine, USA. *Oecologia*, 160, 589–599.
- De Simon, G., Alberti, G., Delle Vedove, G., Zerbi, G., & Peressotti, A. (2012). Carbon stocks and net ecosystem production changes with time in two Italian forest chronosequences. *European Journal of Forest Research*, 131, 1297–1311.
- Dulamsuren, C., Hauck, M., Kopp, G., Ruff, M., & Leuschner, Ch (2017). European beech responds to climate change with growth decline at lower, and growth increase at higher elevations in the center of its distribution range (SW Germany). *Trees*, 3, 673–686 Early View <https://doi.org/10.1007/s00468-016-1499-x>
- Eichhorn, F. (1904). Relationship between stand height and stand growing stock. *Allgemeine Forst-und Jagd-Zeitung*, 80, 45–49 (in German).
- Esper, J., Niederer, R., Bebi, P., & Frank, D. (2008). Climate signal age effects-evidence from young and old trees in the Swiss Engadin. *Forest Ecology and Management*, 255, 3783–3789.
- Eyring, V., Bony, S., Meehl, G. A., Senior, C. A., Stevens, B., Stouffer, R. J., & Taylor, K. E. (2016). Overview of the Coupled Model Intercomparison Project Phase 6 (CMIP6) experimental design and organization. *Geoscientific Model Development*, 9, 1937–1958.
- Ferretti, M., Marchetto, A., Arisci, S., Bussotti, F., Calderisi, M., Carnicelli, S., ... Pompei, E. (2014). On the tracks of Nitrogen deposition effects on temperate forests at their southern European range - an observational study from Italy. *Global Change Biology*, 20, 3423–3438.
- From, F., Lundmark, T., Morling, T., Pommerening, A., & Nordin, A. (2016). Effects of simulated long-term N deposition on *Picea abies* and *Pinus sylvestris* growth in boreal forest. *Canadian Journal of Forest Research*, 46, 1396–1403.
- Gaige, E., Dail, D. B., Hollinger, D. Y., Davidson, E. A., Fernandez, I. J., Sievering, H., ... Halteman, W. (2007). Changes in canopy processes following whole-forest canopy nitrogen fertilization of a mature spruce-hemlock forest. *Ecosystems*, 10, 1133–1147.
- Gelman, A., & Hill, J. (2007). *Data Analysis Using Regression and Multilevel/Hierarchical Models*. Cambridge, UK: Cambridge University Press.
- Gentilescà, T., Vieno, M., Perks, M. P., Borghetti, M., & Mencuccini, M. (2013). Effects of long-term nitrogen addition and atmospheric nitrogen deposition on carbon accumulation in *Picea sitchensis* plantations. *Ecosystems*, 16, 1310–1324.
- Giammarchi, F., Cherubini, P., Pretzsch, H., & Tonon, G. (2017). The increase of atmospheric CO<sub>2</sub> affects growth potential and intrinsic water-use efficiency of Norway spruce forests: insights from a multi-stable isotope analysis in tree rings of two Alpine chronosequences. *Trees - Structure and Function*, 31, 503–515.
- Groenendijk, P., van der Sleen, P., Vlam, M., Bunyavejchewin, S., Bongers, F., & Zuidema, P. A. (2015). No evidence for consistent long-term growth stimulation of 13 tropical tree species: results from tree-ring analysis. *Global Change Biology*, 21, 3762–3776.
- Guerrieri, R., Mencuccini, M., Sheppard, L. J., Saurer, M., Perks, M. P., Levy, P., ... Grace, J. (2011). The legacy of enhanced N and S deposition as revealed by the combined analysis of  $\delta^{13}\text{C}$ ,  $\delta^{18}\text{O}$  and  $\delta^{15}\text{N}$  in tree rings. *Global Change Biology*, 17, 1946–1962.
- Guerrieri, R., Vanguelova, E. L., Michalski, G., Heaton, T. H. E., & Mencuccini, M. (2015). Evidence for the occurrence of biological nitrification and nitrogen deposition processing in forest canopies. *Global Change Biology*, 21, 4613–4626.
- Härdtle, W., Niemeyer, T., Assmann, T., Baiboks, S., Fichtner, A., Friedrich, U., ... von Oheimb, G. (2013). Long-term trends in tree-ring width and isotope signatures ( $\delta^{13}\text{C}$ ,  $\delta^{15}\text{N}$ ) of *Fagus sylvatica* on soils with contrasting water supply. *Ecosystems*, 16, 1413–1428.
- Hastie, T. J., & Tibshirani, R. J. (1990). *Generalized additive models*. London: Chapman and Hall/CRC.
- Hess, C., Niemeyer, T., Fichtner, A., Jansen, K., Kunz, M., Maneke, M., ... Härdtle, W. (2018). Anthropogenic nitrogen deposition alters growth responses of European beech (*Fagus sylvatica* L.) to climate change. *Environmental Pollution*, 233, 92–98.
- Holmes, R. L. (1983). Computer assisted quality control in tree-ring dating and measurement. *Tree Ring Bulletin*, 43, 69–78.
- Hyvönen, R., Ågren, G. I., Linder, S., Persson, T., Cotrufo, M. F., Ekblad, A., ... Wallin, G. (2007). The likely impact of elevated [CO<sub>2</sub>], nitrogen deposition, increased temperature and management on carbon sequestration in temperate and boreal forest ecosystems: a literature review. *New Phytologist*, 173, 463–480.

- IPCC (2014). Climate Change 2014: Impacts, Adaptation, and Vulnerability. Part A: Global and Sectoral Aspects. In C. B. Field, V. R. Barros, D. J. Dokken, K. J. Mach, M. D. Mastrandrea, T. E. Bilir, ... G. V. Yohe (Eds.), *Contribution of Working Group II to the Fifth Assessment Report of the Intergovernmental Panel on Climate Change* (p. 1132). Cambridge, UK and New York, NY: Cambridge University Press.
- Jump, A. S., Hunt, J. M., & Peñuelas, J. (2006). Rapid climate change-related growth decline at the southern range edge of *Fagus sylvatica*. *Global Change Biology*, 12, 2163–2174.
- Kahle, H.P., Karjalainen, T., Schuck, A., Agren, G.I., Kellomäki, S., Mellert, K.H., ... Spiecker, H. (Eds.). (2008). *Causes and consequences of forest growth trends in Europe—Results of the Recognition project* (p. 272). Brill, Leiden: Springer Verlag.
- Kint, V., Aertsen, W., Campioli, M., Vansteenkiste, D., Delcloo, A., & Muys, B. (2012). Radial growth change of temperate tree species in response to altered regional climate and air quality in the period 1901–2008. *Climatic Change*, 115, 343–363.
- Knutzen, F., Dulamsuren, C., Meier, I. C., & Leusche, Ch (2017). Recent climate warming-related growth decline impairs European beech in the center of its distribution. *Ecosystems*, 20, 1494–1511.
- Latte, N., Perin, J., Kint, V., Lebourgeois, F., & Claessens, H. (2016). Major changes in growth rate and growth variability of beech (*Fagus sylvatica* L.) related to soil alteration and climate change in Belgium. *Forests*, 7(8), 174.
- Leonardi, S., Gentilesca, T., Guerrieri, R., Ripullone, F., Magnani, F., Mencuccini, M., ... Borghetti, M. (2012). Assessing the effects of nitrogen deposition and climate on carbon isotope discrimination and intrinsic water-use efficiency of angiosperm and conifer trees under rising CO<sub>2</sub> conditions. *Global Change Biology*, 18, 2925–2944.
- Leonardi, S., Magnani, F., Nolè, A., Van Noije, T., & Borghetti, M. (2015). A global assessment of forest surface albedo and its relationships with climate and atmospheric nitrogen deposition. *Global Change Biology*, 21, 287–298.
- Magnani, F., Grace, J., & Borghetti, M. (2002). Adjustments of tree structure to the environment under hydraulic constraints. *Functional Ecology*, 16, 385–393.
- Magnani, F., Mencuccini, M., Borghetti, M., Berbigier, P., Berninger, F., Delzon, S., ... Grace, J. (2007). The human footprint in the carbon cycle of temperate and boreal forests. *Nature*, 447, 849–851.
- Magnani, F., Mencuccini, M., Borghetti, M., Berninger, F., Delzon, S., Grelle, A., ... Grace, J. (2008). Magnani et al. *Reply Nature*, 451, E3–E4 (14 February 2008).
- McCarroll, D., & Loader, N. J. (2004). Stable isotope in tree rings. *Quaternary Science Reviews*, 23, 771–801.
- Menzel, A., & Fabian, P. (1999). Growing season extended in Europe. *Nature*, 397, 659.
- Mitchell, T. D., & Jones, P. D. (2005). An improved method of constructing a database of monthly climate observations and associated high-resolution grids. *International Journal of Climatology*, 25(6), 693–712.
- Nakagawa, S., & Schielzeth, H. (2013). A general and simple method for obtaining R<sup>2</sup> from generalized linear mixed-effects models. *Methods in Ecology and Evolution*, 4, 133–142.
- New, M., Hulme, M., & Jones, P. (2000). Representing twentieth-century space-time climate variability. Part II: Development of 1901–96 monthly grids of terrestrial surface climate. *Journal of Climate*, 13, 2217–2238.
- Peñuelas, J., Canadell, J. G., & Ogaya, R. (2011). Increased water-use efficiency during the 20th century did not translate into enhanced tree growth. *Global Ecology and Biogeography*, 20, 597–608.
- Pignatti, S. (1998). *I boschi d'Italia. Sinecologia e biodiversità*. Torino, Italy: UTET, 680 p..
- Piovesan, G., Biondi, F., Di Filippo, A., Alessandrini, A., & Maugeri, M. (2008). Drought-driven growth reduction in old beech (*Fagus sylvatica*) forests of the central Apennines, Italy. *Global Change Biology*, 14, 1265–1281.
- Pregitzer, K. S., Burton, A. J., Zak, D. R., & Talhelm, A. F. (2008). Simulated chronic nitrogen deposition increases carbon storage in Northern Temperate forests. *Global Change Biology*, 14, 142–153.
- Pretzsch, H., Biber, P., Schütze, G., Uhl, E., & Rötzer, U. (2014). Forest stand growth dynamics in Central Europe have accelerated since 1870. *Nature Communications*, 5, 4967.
- R Development Core Team (2015). *R A Language and Environment for Statistical Computing*. Vienna Austria: R Foundation for Statistical Computing URL: <http://www.Rproject.org>.
- Rubino, D., & McCarthy, B. C. (2004). Comparative analysis of dendroecological methods used to assess disturbance events. *Dendrochronologia*, 21, 97–115.
- Ryan, M. G., Binkley, D., & Fownes, J. H. (1997). Age-related decline in forest productivity: pattern and process. *Advances in Ecological Research*, 27, 213–262.
- Schielzeth, H. (2010). Simple means to improve the interpretability of regression coefficients. *Methods in Ecology and Evolution*, 2, 103–113.
- Schlesinger, W. H. (2009). On the fate of anthropogenic nitrogen. *Proceedings of the National Academy of Sciences USA*, 106, 203–208.
- Schulte-Uebbing, L., & de Vries, W. (2017). Global-scale impacts of nitrogen deposition on tree carbon sequestration in tropical, temperate, and boreal forests: A meta-analysis. *Global Change Biology*, 24, 1–16. <https://doi.org/10.1111/gcb.13862>
- Sievering, H., Tomaszewski, T., & Torizzo, J. (2007). Canopy uptake of atmospheric N deposition at a conifer forest. Part I - Canopy N budget, photosynthetic efficiency and net ecosystem exchange. *Tellus Series B*, 59, 483–492.
- Silva, L. C. R., & Anand, M. (2013). Probing for the influence of atmospheric CO<sub>2</sub> and climate change on forest ecosystems across biomes. *Global Ecology and Biogeography*, 22, 83–92.
- Skovsgaard, J. P., & Vanclay, K. (2008). Forest site productivity: a review of the evolution of dendrometric concepts for even-aged stands. *Forestry (Lond)*, 81, 13–31.
- Solberg, S., Andreassen, K., Clarke, N., Tørseth, K., Tveito, O. E., Strand, G.-H., & Tomter, S. (2004). The possible influence of nitrogen and acid deposition on forest growth in Norway. *Forest Ecology and Management*, 192, 241–249.
- Solberg, S., Dobbertin, M., Reinds, G. J., Lange, H., Andreassen, K., Fernandez, P. G., ... de Vries, W. (2009). Analyses of the impact of changes in atmospheric deposition and climate on forest growth in European monitoring plots: A stand growth approach. *Forest Ecology and Management*, 258, 1735–1750.
- Sparks, J. D. (2009). Ecological ramifications of the direct foliar uptake of nitrogen. *Oecologia*, 159, 1–13.
- Spiecker, H. (1995). Growth dynamics in a changing environment - long-term observations. *Plant and Soil*, 169, 565–561.
- Spiecker, H., Mielikäinen, K., Köhl, M., & Skovsgaard, J.P., (Eds.). (1996). *Growth trends in European Forests. Research report 5, European Forest Institute*. Berlin: Springer 372 p.
- Stephenson, N. L., Das, A. J., Condit, R., Russo, S. E., Baker, P. J., Beckman, N. G., ... Zavala, M. A. (2014). Rate of tree carbon accumulation increases continuously with tree size. *Nature*, 507, 90–93.
- Tegel, W., Seim, A., Hakelberg, D., Hoffmann, S., Panev, M., Westphal, T., & Buntgen, U. (2014). A recent growth increase of European beech (*Fagus sylvatica* L.) at its Mediterranean distribution limit contradicts drought stress. *European Journal of Forest Research*, 133, 61–71.
- Vadeboncoeur, M. A. (2010). Meta-analysis of fertilization experiments indicates multiple limiting nutrients in northeastern deciduous forests. *Canadian Journal of Forest Research*, 40, 1766–1780.
- Venter, M., Dwyer, J., Dieleman, W., Ramachandra, A., Gillieson, D., Laurance, S., ... Bird, M. I. (2017). Optimal climate for large trees at high elevations drives patterns of biomass in remote forests of Papua New Guinea. *Global Change Biology*, 23, 4873–4883 Early View Article, <https://doi.org/10.1111/gcb.13741>

- Vicente-Serrano, S. M., Beguería, S., & López-Moreno, J. I. (2010). A Multi-scalar drought index sensitive to global warming: The Standardized Precipitation Evapotranspiration Index – SPEI. *Journal of Climate*, 23, 1696.
- de Vries, W., Dobbertin, M. H., Solberg, S., Van Dobbers, H. F., & Schaub, M. (2014). Impacts of acid deposition, ozone exposure and weather conditions on forest ecosystems in Europe: an overview. *Plant and Soil*, 380, 1–45.
- de Vries, W., Reinds, G. J., Guindersen, P., & Sterba, H. (2006). The impact of nitrogen deposition on carbon sequestration in European forests and forest soils. *Global Change Biology*, 12, 1151–1173.
- de Vries, W., Solberg, S., Dobbertin, M., Sterba, H., Laubhahn, D., Reinds, G.J., ... Sutton, M.A. (2008). Ecologically implausible carbon response? *Nature*, 451, E1–E3 (14 February 2008). <https://doi.org/10.1038/nature06579>
- de Vries, W., Solberg, S., Dobbertin, M., Sterba, H., Laubhahn, D., van Oijen, M., ... Sutton, M. A. (2009). The impact of nitrogen deposition on carbon sequestration by European forests and heathlands. *Forest Ecology and Management*, 258, 1814–1823.
- Wood, S.N. (2006). *Generalized Additive Models: An Introduction with R*. Boca Raton, FL: Chapman and Hall/CRC.
- Xu, C.-Y., Turnbull, M. H., Tissue, D. T., Lewis, J. D., Carson, R., Schuster, W. S. F., ... Griffin, K. L. (2012). Age-related decline of stand biomass accumulation is primarily due to mortality and not to reduction in NPP associated with individual tree physiology, tree growth or stand structure in a *Quercus*-dominated forest. *Journal of Ecology*, 100, 428–440.
- Zang, C., Hartl-Meier, C., Dittmar, C., Rothe, A., & Menzel, A. (2014). Patterns of drought tolerance in major European temperate forest trees: climatic drivers and levels of variability. *Global Change Biology*, 20, 3767–3779.
- Zhang, W., Shen, W., Zhu, S., Wan, S., Luo, Y., Yan, J., ... Fu, S. (2015). CAN canopy addition of nitrogen better illustrate the effect of atmospheric nitrogen deposition on forest ecosystem? *Scientific Reports*, 5, 11245.

## SUPPORTING INFORMATION

Additional Supporting Information may be found online in the supporting information tab for this article.

**How to cite this article:** Gentilesca T, Rita A, Brunetti M, et al. Nitrogen deposition outweighs climatic variability in driving annual growth rate of canopy beech trees: Evidence from long-term growth reconstruction across a geographic gradient. *Glob Change Biol*. 2018;00:1–15. <https://doi.org/10.1111/gcb.14142>